

# Genomic Sequencing of Cancer-related Genes in Sinonasal Squamous Cell Carcinoma and Coexisting Inverted Papilloma

RYUTARO UCHI<sup>1,2</sup>, RINA JIROMARU<sup>1,3</sup>, RYUJI YASUMATSU<sup>1</sup>, HIDETAKA YAMAMOTO<sup>3</sup>,  
TAKAHIRO HONGO<sup>1,3</sup>, TOMOMI MANAKO<sup>1</sup>, KUNIAKI SATO<sup>1</sup>, KAZUKI HASHIMOTO<sup>1</sup>,  
TAKAHIRO WAKASAKI<sup>1</sup>, MIOKO MATSUO<sup>1</sup> and TAKASHI NAKAGAWA<sup>1</sup>

<sup>1</sup>Department of Otorhinolaryngology, Graduate School of Medical Sciences, Kyushu University, Fukuoka, Japan;

<sup>2</sup>Division of Otorhinolaryngology and Head and Neck Surgery, National Kyushu Medical Center, Fukuoka, Japan;

<sup>3</sup>Department of Anatomic Pathology, Graduate School of Medical Sciences, Kyushu University, Fukuoka, Japan

**Abstract.** *Background:* The genetic basis of sinonasal inverted papilloma (SNIP)-derived squamous cell carcinoma (SCC) has not yet been well characterized. *Aim:* To characterize the genetic abnormalities of SNIP and SNIP-derived SCC and to uncover their differences. *Materials and Methods:* Mutations of 409 genes were analyzed using amplicon targeted sequencing in a total of six papilloma/carcinoma samples from four patients with SNIP-derived SCC. *Results:* The genes that were mutated in multiple cases were epidermal growth factor receptor (EGFR) (3/6), cyclin-dependent kinase inhibitor 2A (CDKN2A) (3/6), lysine methyltransferase 2D (KMT2D) (3/6), tumor protein p53 (TP53) (3/6), neurofibromin 1 (NF1) (3/6), phosphodiesterase 4D interacting protein (PDE4DIP) (3/6), cytochrome P450 family 2 subfamily D member 6 (CYP2D6) (2/6), fms-related receptor tyrosine kinase 4 (FLT4) (2/6) and myosin heavy chain 9 (MYH9) (2/6). Of the two cases analyzed in the papilloma–oncology carcinoma pair, one did not have any common mutations; the other showed a staged functional deletion of TP53 during the process of malignant transformation from SNIP to SCC. *Conclusion:* CDKN2A, KMT2D, NF1, PDE4DIP, CYP2D6, FLT4, and MYH9 were identified as candidate novel SNIP-derived SCC-related genes.

Sinonasal papillomas are generally considered benign tumors that can be cured by endoscopic surgery and are classified by the World Health Organization into three types: Inverted papilloma (IP), exophytic papilloma and oncocytic papilloma (1, 2). The most common type of papilloma is IP, with an

incidence of 0.74-1.5 cases per 100,000 population per year (3). Sinonasal inverted papilloma (SNIP) is associated with squamous cell carcinoma (SCC), either synchronously or metachronously (4). The rate of carcinoma is reportedly 5 to 10% and is considered to be malignantly transformed from papilloma (5-7). SNIP-derived SCC has the same poor prognosis as de novo sinonasal SCC, with a reported 5-year postoperative survival rate of 39.6-65.7% (8-10). The preoperative diagnosis of malignant transformation of SNIP is important for radical resection. Improved tools that facilitate the preoperative diagnosis of SCC complications is a clinical issue that needs to be addressed, as imaging and markers are not well established (5, 11, 12).

The mechanism of SNIP development and its malignant transformation remain largely unknown (5). Immunohistological studies and studies focusing on certain genes have searched for risk factors for SNIP associated with SCC (13-16). In recent years, comprehensive genetic analyses using next-generation sequencing have become available and have revealed the genetic background of many carcinoma types; however, few genome-wide analyses of papilloma-derived cancer have been performed (17). Furthermore, in other types of cancer, the accumulation of genetic abnormalities during cancer evolution has been reported by comparing genetic abnormalities in precancerous and benign tumors with cancerous lesions using next-generation sequencing (18).

In this study, we identified genes that may be involved in the development of papilloma-derived SCC by analyzing the genomes of both papilloma and SCC components in papilloma-derived SCC specimens

*Correspondence to:* Ryuji Yasumatsu, MD, Ph.D., Department of Otorhinolaryngology, Graduate School of Medical Sciences, Kyushu University, 3-1-1 Higashi-ku, Fukuoka, 812-8582, Japan. E-mail: yasuryuj@qent.med.kyushu-u.ac.jp

**Key Words:** Sinonasal papilloma, squamous cell carcinoma, head and neck cancer, target sequencing.

## Materials and Methods

**Ethics statement.** The protocol of this study was reviewed and approved by the Institutional Review Boards and Ethics Committees of Kyushu University (Protocol Number: 700-2 and 30-268). All procedures with human samples were conducted according to the principles expressed in the Declaration of Helsinki.

Table I. The clinicopathological characteristics of patients with sinonasal inverted papilloma (IP)/squamous cell carcinoma (SCC).

| Case no. | Sample type | Age, years | Gender | Primary site    | TNM stage* |
|----------|-------------|------------|--------|-----------------|------------|
| 7        | SCC         | 66         | Female | Maxillary sinus | T2N0M0     |
| 10       | IP          | 85         | Male   | Frontal sinus   | T4aN0M0    |
| 16       | IP, SCC     | 83         | Female | Maxillary sinus | T2N0M0     |
| 17       | IP, SCC     | 64         | Male   | Nasal cavity    | T4bN2bM0   |

\*According to the eighth edition of the TNM Classification of Malignant Tumors (26).

**Patients.** Four cases of mixed SNIP and SCC that were pathologically diagnosed at the Department of Otolaryngology, Kyushu University Hospital, between 2014 and 2019 were included in this study (Table I).

**DNA extraction.** Formalin-fixed and paraffin-embedded specimens of surgically resected tumor samples were separated into papilloma and SCC parts using a laser microdissection method with a Leica Laser Microdissection System (Leica Microsystems, Wetzlar, Germany); papilloma and SCC were distinguished based on the diagnosis of the pathologist (Figure 1). The extraction of genomic DNA from the formalin-fixed and paraffin-embedded tissue was conducted using QIAamp DNA Micro Kit (Qiagen, Chatsworth, CA, USA). In two cases (number 16 and 17), both the papilloma and the cancerous part of the sample were extractable but in another two (cases 10 and 7), DNA was only obtained from the papilloma and the cancerous part of the sample, respectively. Thus, we sequenced three samples of the papilloma and three samples of the cancerous part.

**Targeted sequencing.** Library preparation from the extracted DNA and targeted exome sequencing were performed at Cell Innovator (Fukuoka, Japan). DNA was subjected to targeted exome sequencing using an Ion AmpliSeq™ Comprehensive Cancer Panel (ThermoFisher, Waltham, MA, USA). The 409 genes included in the panel are shown in Table II. The obtained sequences were called for mutations with a mutation rate of >5% using SNPEff ver4.1 (19). Among the identified mutations, insertion, deletion and non-synonymous single nucleotide variants listed in the COSMIC Cancer Gene Census (Sanger Institute, Hinxton, UK) were considered mutant genes. Single nucleotide polymorphisms (SNPs) registered in dbSNP141 and 142 were excluded. We also excluded mutations at the same position and of the same form observed in at least three out of the four cases as sequencing errors.

**Confirmation of the same case by SNP.** Of the six samples from four cases, two were samples of paired SNIP and SCC. To confirm that the samples were paired without mismatch, the match rate of the SNPs identified as mutations was checked among the samples. The match rate was defined as the product set of SNPs/sum set of SNPs.

## Results

The number of detected mutations ranged from 2-20 mutations per sample, with an average of 14 mutations per sample (Table III). All mutations are described in Table IV. The average

numbers of indel and nonsense mutations were 4.9 and 3.5, respectively; missense mutations registered in COSMIC were only found in two genes, *EGFR* and *CDKN2A*, in case 7 SCC. The number of mutations in the IP and SCC components did not differ to a statistically significant extent.

The nine genes that were mutated in multiple cases were epidermal growth factor receptor (*EGFR*) (3/6), cyclin-dependent kinase inhibitor 2A (*CDKN2A*) (3/6), lysine methyltransferase 2D (*KMT2D*) (3/6), tumor protein p53 (*TP53*) (3/6), neurofibromin 1 (*NF1*) (3/6), phosphodiesterase 4D interacting protein (*PDE4DIP*) (3/6), cytochrome P450 family 2 subfamily D member 6 (*CYP2D6*) (2/6), fms-related receptor tyrosine kinase 4 (*FLT4*) (2/6) and myosin heavy chain 9 (*MYH9*) (2/6) (Figure 2). Among these, *KMT2D* and *TP53* mutations were found in two positions in the samples of case 7 SCC and case 17 IP, respectively. Among the recurrent mutations, there were no mutations specifically common to the three SCCs when they were compared to the three IP parts.

The SCC and IP areas within the same case were sequenced in cases 16 and 17. Confirmation of SNPs detected in cases 16 and 17 showed that the average SNP concordance rate between samples of different cases was 55%, while the concordance rate between papilloma and SCC within the same case was 96.2% and 98.0% for cases 16 and 17, respectively. Each of the tumors was confirmed to have originated from the same germline (Figure 3). Although confirmed to have originated from the same germline, none of the mutations were common to the SCC and IP components in case 16 (Figure 4).

On the other hand, in case 17, the SCC and IP had five common mutations: six SCC-specific mutations and three IP-specific mutations. Both SCC and IP of case 17 had mutations in *TP53*, p.Val73fs was common to both, while p.Glu339\* was only found in case 17 SCC. In addition to *TP53* (p.Glu339\*), five mutations, collagen type I alpha 1 chain (*COL1A1*), XPA DNA damage recognition and repair factor (*XPA*), SRY-box transcription factor 11 (*SOX11*), *CYP2D6*, and *FLT4*, were found to be specific to SCC in case 17. A *CYP2D6* mutation was also found in SCC of case 7, suggesting that mutation of *CYP2D6* may contribute to the malignant transformation of SNIP.

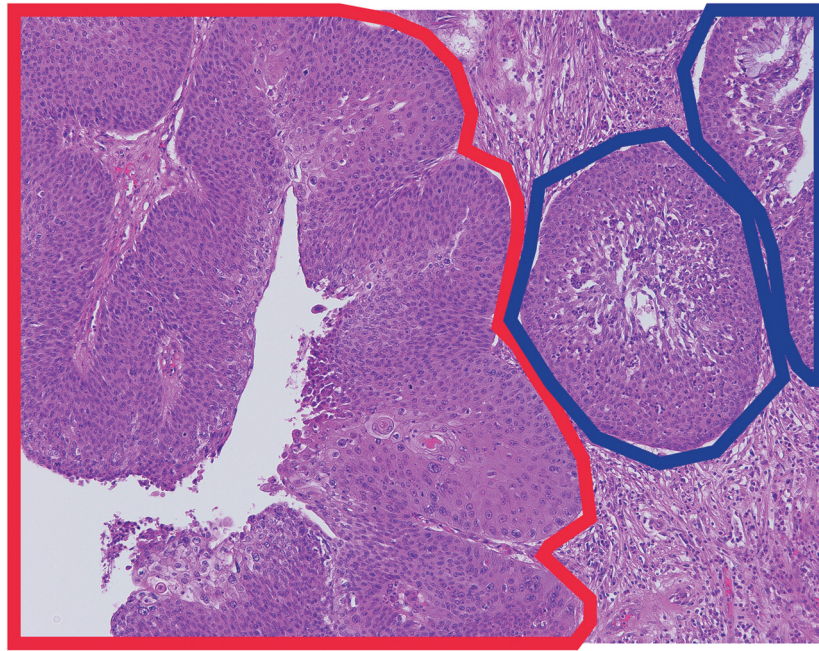


Figure 1. Laser micro dissection to separate papilloma and carcinoma. Hematoxylin-eosin staining of sinonasal inverted papilloma-derived squamous cell carcinoma is shown ( $\times 200$ ). Separation of cancerous (red) and papilloma (blue) areas was performed by microdissection.

Table II. The gene list of target sequence.

|          |         |         |        |         |          |        |        |        |         |         |         |          |        |
|----------|---------|---------|--------|---------|----------|--------|--------|--------|---------|---------|---------|----------|--------|
| ABL1     | BCL2    | CDH20   | DDB2   | EXT1    | GATA2    | ING4   | MAFB   | MSH6   | NSD1    | PKHD1   | RNF2    | STK36    | TRIP11 |
| ABL2     | BCL2L1  | CDH5    | DDIT3  | EXT2    | GATA3    | IRF4   | MAGEA1 | MTOR   | NTRK1   | PLAG1   | RNF213  | SUFU     | TRRAP  |
| ACVR2A   | BCL2L2  | CDK12   | DDR2   | EZH2    | GDNF     | IRS2   | MAGI1  | MTR    | NTRK3   | PLCG1   | ROS1    | SYK      | TSC1   |
| ADAMTS20 | BCL3    | CDK4    | DEK    | FAM123B | GNAI1    | ITGA10 | MALT1  | MTRR   | NUMA1   | PLEKHG5 | RPS6KA2 | SYNE1    | TSC2   |
| AFF1     | BCL6    | CDK6    | DICER1 | FANCA   | GNAQ     | ITGA9  | MAML2  | MUC1   | NUP214  | PML     | RRM1    | TAF1     | TSHR   |
| AFF3     | BCL9    | CDK8    | DNMT3A | FANCC   | GNAS     | ITGB2  | MAP2K1 | MUTYH  | NUP98   | PMS1    | RUNX1   | TAF1L    | UBR5   |
| AKAP9    | BCR     | CDKN2A  | DPYD   | FANCD2  | GPR124   | ITGB3  | MAP2K2 | MYB    | PAK3    | PMS2    | RUNX1T1 | TAL1     | UGT1A1 |
| AKT1     | BIRC2   | CDKN2B  | DST    | FANCF   | GRM8     | JAK1   | MAP2K4 | MYC    | PALB2   | POU5F1  | SAMD9   | TBX22    | USP9X  |
| AKT2     | BIRC3   | CDKN2C  | EGFR   | FANCG   | GUCY1A2  | JAK2   | MAP3K7 | MYCL1  | PARP1   | PPARG   | SBDS    | TCF12    | VHL    |
| AKT3     | BIRC5   | CEBPA   | EML4   | FAS     | HCAR1    | JAK3   | MAPK1  | MYCN   | PAX3    | PPP2R1A | SDHA    | TCF3     | WAS    |
| ALK      | BLM     | CHEK1   | EP300  | FBXW7   | HIF1A    | JUN    | MAPK8  | MYD88  | PAX5    | PRDM1   | SDHB    | TCF7L1   | WHSC1  |
| APC      | BLNK    | CHEK2   | EP400  | FGFR1   | HLF      | KAT6A  | MARK1  | MYH11  | PAX7    | PRKAR1A | SDHC    | TCF7L2   | WRN    |
| AR       | BMPRI1A | CIC     | EPHA3  | FGFR2   | HNF1A    | KAT6B  | MARK4  | MYH9   | PAX8    | PRKDC   | SDHD    | TCL1A    | WT1    |
| ARID1A   | BRAF    | CKS1B   | EPHA7  | FGFR3   | HOOK3    | KDM5C  | MBD1   | NBN    | PBRM1   | PSIP1   | SEP9    | TET1     | XPA    |
| ARID2    | BRD3    | CMPK1   | EPHB1  | FGFR4   | HRAS     | KDM6A  | MCL1   | NCOA1  | PBX1    | PTCH1   | SETD2   | TET2     | XPC    |
| ARNT     | BRIP1   | COL1A1  | EPHB4  | FH      | HSP90AA1 | KDR    | MDM2   | NCOA2  | PDE4DIP | PTEN    | SF3B1   | TFE3     | XPO1   |
| ASXL1    | BTB     | CRBN    | EPHB6  | FLCN    | HSP90AB1 | KEAP1  | MDM4   | NCOA4  | PDGFB   | PTGS2   | SGK1    | TGFBF2   | XRCC2  |
| ATF1     | BUB1B   | CREB1   | ERBB2  | FLI1    | ICK      | KIT    | MEN1   | NF1    | PDGFRA  | PTPN11  | SH2D1A  | TGM7     | ZNF384 |
| ATM      | CARD11  | CREBBP  | ERBB3  | FLT1    | IDH1     | KLF6   | MET    | NF2    | PDGFRB  | PTPRD   | SMAD2   | THBS1    | ZNF521 |
| ATR      | CASC5   | CRKL    | ERBB4  | FLT3    | IDH2     | KRAS   | MITF   | NFE2L2 | PER1    | PTPRT   | SMAD4   | TIMP3    |        |
| ATRX     | CBL     | CRTC1   | ERCC1  | FLT4    | IGF1R    | LAMP1  | MLH1   | NFKB1  | PGAP3   | RAD50   | SMARCA4 | TLR4     |        |
| AURKA    | CCND1   | CSF1R   | ERCC2  | FN1     | IGF2     | LCK    | MLL    | NFKB2  | PHOX2B  | RAF1    | SMARCB1 | TLX1     |        |
| AURKB    | CCND2   | CSMD3   | ERCC3  | FOXL2   | IGF2R    | LIFR   | MLL2   | NIN    | PIK3C2B | RALGDS  | SMO     | TNFAIP3  |        |
| AURKC    | CCNE1   | CTNNA1  | ERCC4  | FOXO1   | IKBKB    | LPHN3  | MLL3   | NKX2-1 | PIK3CA  | RARA    | SMUG1   | TNFRSF14 |        |
| AXL      | CD79A   | CTNNB1  | ERCC5  | FOXO3   | IKBKE    | POT1   | MLLT10 | NLRP1  | PIK3CB  | RB1     | SOC3    | TNK2     |        |
| BAI3     | CD79B   | CYLD    | ERG    | FOXP1   | IKZF1    | LPP    | MMP2   | NOTCH1 | PIK3CD  | RECQL4  | SOX11   | TOP1     |        |
| BAP1     | CDC73   | CYP2C19 | ESR1   | FOXP4   | IL2      | LRP1B  | MN1    | NOTCH2 | PIK3CG  | REL     | SOX2    | TP53     |        |
| BCL10    | CDH1    | CYP2D6  | ETS1   | FZR1    | IL21R    | LTF    | MPL    | NOTCH4 | PIK3R1  | RET     | SRC     | TPR      |        |
| BCL11A   | CDH11   | DAXX    | ETV1   | G6PD    | IL6ST    | LTK    | MRE11A | NPM1   | PIK3R2  | RHOH    | SSX1    | TRIM24   |        |
| BCL11B   | CDH2    | DCC     | ETV4   | GATA1   | IL7R     | MAF    | MSH2   | NRAS   | PIM1    | RNASEL  | STK11   | TRIM33   |        |

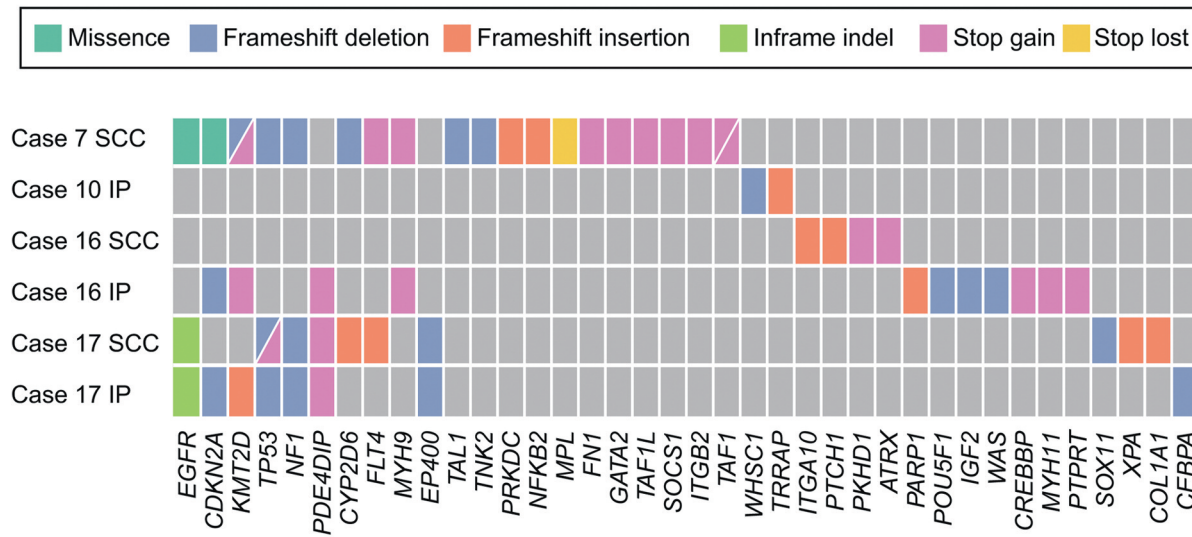


Figure 2. Overview of mutations in sinonasal inverted papilloma (SNIP) and SNIP-derived squamous cell carcinoma (SCC). All mutated genes in SNIP and SNIP-derived SCC were color coded according to mutation type. Gene designations are given below Table III.

Table III. The number of mutations found in six tissue samples of inverted papilloma (IP)/squamous cell carcinoma (SCC) from four cases.

| Case no. | Mutation type, n |          |               |                  |           |           |
|----------|------------------|----------|---------------|------------------|-----------|-----------|
|          | Histology        | Missense | Inframe indel | Frameshift indel | Stop gain | Stop lost |
| 7        | SCC              | 2        | 0             | 8                | 10        | 1         |
| 10       | IP               | 0        | 0             | 2                | 0         | 0         |
| 16       | SCC              | 0        | 0             | 2                | 2         | 0         |
|          | IP               | 0        | 0             | 5                | 6         | 0         |
| 17       | SCC              | 0        | 1             | 8                | 2         | 0         |
|          | IP               | 0        | 1             | 6                | 1         | 0         |

## Discussion

Radical surgical resection of papilloma-derived cancer is important for good treatment outcomes; however, complications of cancer are difficult to predict before surgery, and the discovery of markers that predict cancer complications is desired (10). Immunohistological approaches and single gene sequencing of papilloma-derived cancer suggested that *TP53* and *EGFR* abnormalities may be common findings in complicated cancer cases (15, 20). A previous study of 26 genes by Yasukawa *et al.* identified *TP53*, G protein subunit alpha q (*GNAQ*), platelet-derived growth factor receptor alpha (*PDGFRA*), *EGFR*, phosphatidylinositol-4,5-bisphosphate 3-kinase catalytic subunit alpha (*PIK3CA*), *KRAS* proto-oncogene GTPase (*KRAS*), APC regulator of WNT signaling pathway (*APC*), serine/threonine kinase 11 (*STK11*), and mutS homolog 6 (*MSH6*) as recurrent mutations in papilloma and papilloma-derived carcinoma by target sequencing. Among them, *KRAS* mutation is cancer-

specific and may be a gene mutation involved in malignant transformation (17). In this study, we performed a comprehensive mutation analysis using cancer panel gene sequencing on three cancer and three papilloma samples from four papilloma-derived cancer cases. A total of 409 genes were targeted, covering most of the mutations analyzed in previous studies. In this study, we found mutations in *EGFR* and *TP53* from among those identified in previous studies. Furthermore, we found that *CDKN2A*, *KMT2D*, *NF1*, *PDE4DIP*, *CYP2D6*, *FLT4*, and *MYH9* were mutated in more than one case, suggesting that they may be involved in the development of SNIP and SNIP-derived SCC. Among these genes, *CDKN2A* exhibited a loss of function in more than 50% of head and neck squamous cell carcinomas of the pharynx and larynx, and may have an important role in the development and oncogenesis of SNIP-derived SCC (21). On the other hand, we did not find *KRAS* mutation, although Yasukawa *et al.* reported that it may be associated with malignant transformation of SNIP (17).

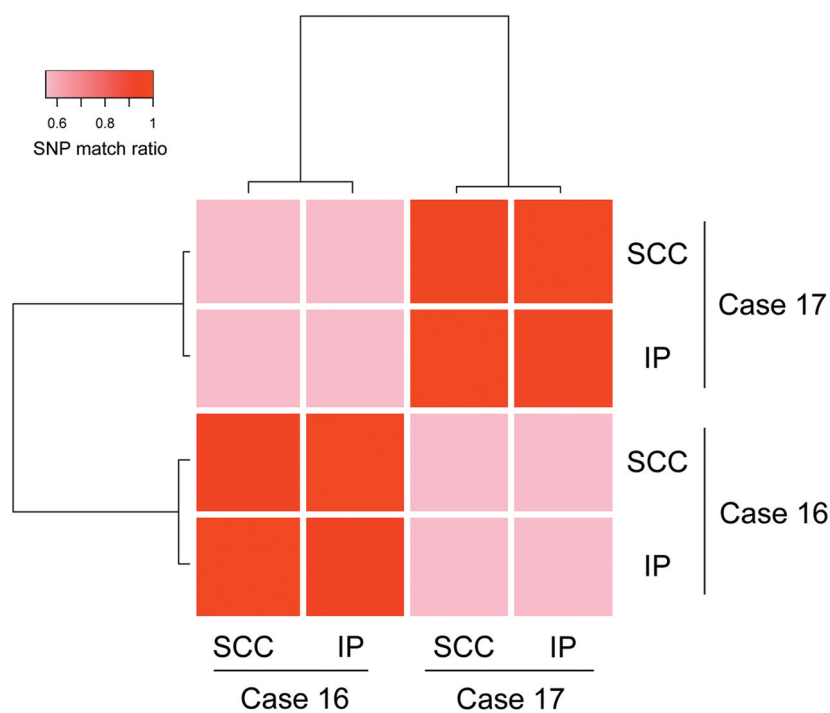


Figure 3. Correlation of single nucleotide polymorphisms (SNPs) in cases 16 and 17. The heat map shows the match rate of SNPs detected in each sample by sequencing.

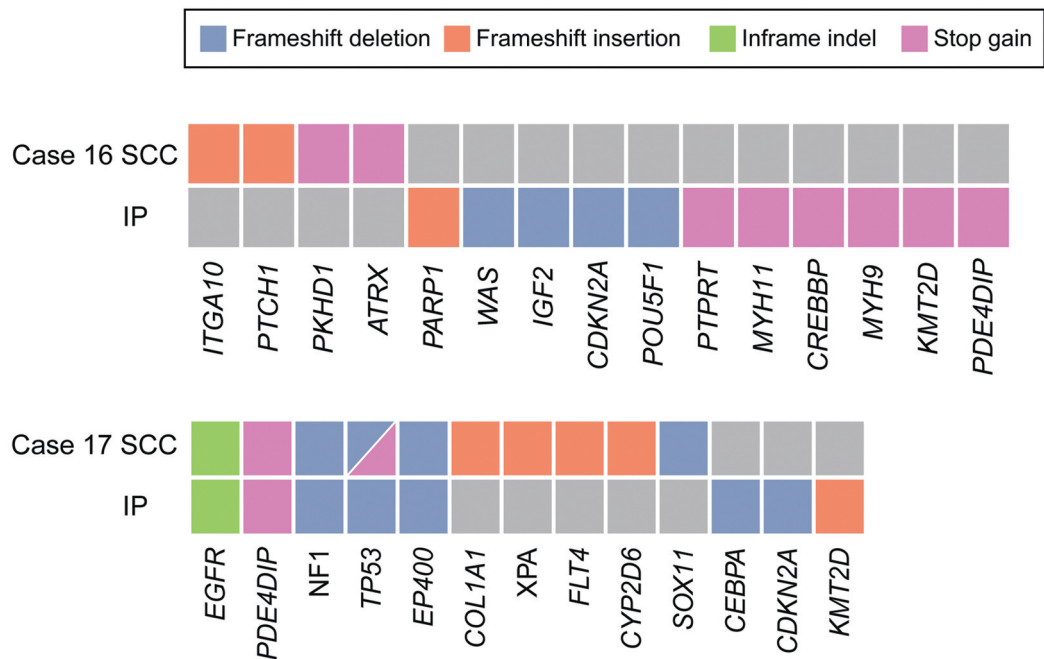


Figure 4. Comparison of sinonasal inverted papilloma (SNIP) and SNIP-derived squamous cell carcinoma (SCC) mutations within the same case. SNIP and SNIP-derived SCC mutations were compared in cases 16 and 17. Gene designations are given below Table IV.

Table IV. Information on mutations found in samples of inverted papilloma (IP)/squamous cell carcinoma (SCC) from six samples from four cases.

| Case no. | Histology | Gene name      | Chrom | Position  | Reference      | Alteration    | Annotation                         | HGVS.c                   | HGVS.p                       | COSMIC ID |
|----------|-----------|----------------|-------|-----------|----------------|---------------|------------------------------------|--------------------------|------------------------------|-----------|
| 7        | SCC       | <i>MPL</i>     | chr1  | 43818443  | A              | G             | stop_lost                          | c.1908A>G                | p.Ter636Trpext*?             | .         |
|          |           | <i>TAL1</i>    | chr1  | 47685569  | GC             | G             | frameshift_variant                 | c.818delG                | p.Gly273fs                   | .         |
|          |           | <i>FN1</i>     | chr2  | 216293010 | C              | T             | stop_gained                        | c.737G>A                 | p.Trp246*                    | .         |
|          |           | <i>GATA2</i>   | chr3  | 128205845 | C              | T             | stop_gained                        | c.30G>A                  | p.Trp10*                     | .         |
|          |           | <i>TNK2</i>    | chr3  | 195595228 | CGGGGG         | CGGGG         | frameshift_variant                 | c.2125delC               | p.Pro710fs                   | .         |
|          |           | <i>FLT4</i>    | chr5  | 180047969 | G              | A             | stop_gained                        | c.2206C>T                | p.Gln736*                    | .         |
|          |           | <i>EGFR</i>    | chr7  | 55249010  | G              | A             | missense_variant                   | c.2308G>A                | p.Asp770Asn                  | COSM14068 |
|          |           | <i>PRKDC</i>   | chr8  | 48805816  | A              | AG            | frameshift_variant                 | c.3729dupC               | p.Phe1244fs                  | .         |
|          |           | <i>CDKN2A</i>  | chr9  | 21971159  | C              | T             | missense_variant                   | c.199G>A                 | p.Gly67Ser                   | COSM12746 |
|          |           | <i>TAF1L</i>   | chr9  | 32631839  | G              | A             | stop_gained                        | c.3739C>T                | p.Gln1247*                   | .         |
|          |           | <i>TAF1L</i>   | chr9  | 32632938  | C              | T             | stop_gained                        | c.2640G>A                | p.Trp880*                    | .         |
|          |           | <i>NFKB2</i>   | chr10 | 104159195 | C              | CG            | frameshift_variant                 | c.1268_1269insG          | p.Ser424fs                   | .         |
|          |           | <i>KMT2D</i>   | chr12 | 49427621  | G              | A             | stop_gained                        | c.10867C>T               | p.Gln3623*                   | .         |
|          |           | <i>KMT2D</i>   | chr12 | 49445148  | TG             | T             | frameshift_variant                 | c.2317delC               | p.Gln773fs                   | .         |
|          |           | <i>SOCS1</i>   | chr16 | 11348813  | G              | A             | stop_gained                        | c.523C>T                 | p.Gln175*                    | .         |
|          |           | <i>TP53</i>    | chr17 | 7579470   | CGG            | CG            | frameshift_variant                 | c.215delC                | p.Val73fs                    | COSM46307 |
|          |           | <i>NF1</i>     | chr17 | 29553477  | ACCCC<br>CCCCG | ACCCC<br>CCG  | frameshift_variant                 | c.2033delC               | p.Pro678fs                   | COSM24489 |
|          |           | <i>ITGB2</i>   | chr21 | 46306657  | C              | T             | stop_gained                        | c.2241G>A                | p.Trp747*                    | .         |
|          |           | <i>MYH9</i>    | chr22 | 36710279  | G              | A             | stop_gained                        | c.1465C>T                | p.Gln489*                    | .         |
|          |           | <i>CYP2D6</i>  | chr22 | 42525755  | CG             | C             | frameshift_variant                 | c.336delC                | p.Phe112fs                   | .         |
| 10       | IP        | <i>TAF1</i>    | chrX  | 70643066  | C              | T             | stop_gained                        | c.4612C>T                | p.Gln1538*                   | .         |
|          |           | <i>WHSC1</i>   | chr4  | 1980558   | GC             | G             | frameshift_variant                 | c.4028delC               | p.Pro1343fs                  | .         |
| 16       | SCC       | <i>TRRAP</i>   | chr7  | 98508875  | C              | CA            | frameshift_variant                 | c.1994dupA               | p.Asn665fs                   | .         |
|          |           | <i>ITGA10</i>  | chr1  | 145527980 | G              | GT            | frameshift_variant                 | c.220dupT                | p.Tyr74fs                    | .         |
| 17       | SCC       | <i>PKHD1</i>   | chr6  | 51720839  | A              | C             | stop_gained                        | c.7763T>G                | p.Leu2588*                   | .         |
|          |           | <i>PTCH1</i>   | chr9  | 98278956  | G              | GT            | frameshift_variant                 | c.146dupA                | p.Asn49fs                    | .         |
|          |           | <i>ATRX</i>    | chrX  | 76937750  | T              | A             | stop_gained                        | c.2998A>T                | p.Lys1000*                   | .         |
|          |           | <i>PDE4DIP</i> | chr1  | 144915561 | G              | A             | stop_gained                        | c.1864C>T                | p.Arg622*                    | .         |
|          |           | <i>PARP1</i>   | chr1  | 226570839 | G              | GC            | frameshift_variant                 | c.1056_1057insG          | p.Gln353fs                   | .         |
|          |           | <i>POU5F1</i>  | chr6  | 31138041  | AG             | A             | frameshift_variant                 | c.356delC                | p.Pro119fs                   | .         |
|          |           | <i>CDKN2A</i>  | chr9  | 21971083  | TCC            | TC            | frameshift_variant                 | c.273delG                | p.Asp92fs                    | COSM13623 |
|          |           | <i>IGF2</i>    | chr11 | 2154241   | TGGGG<br>GGGC  | TGGGG<br>GGC  | frameshift_variant                 | c.680delC                | p.Pro229fs                   | .         |
|          |           | <i>KMT2D</i>   | chr12 | 49445068  | G              | A             | stop_gained                        | c.2398C>T                | p.Gln800*                    | .         |
|          |           | <i>CREBBP</i>  | chr16 | 3778612   | G              | A             | stop_gained                        | c.6436C>T                | p.Gln2146*                   | .         |
|          | IP        | <i>MYH11</i>   | chr16 | 15814848  | G              | A             | stop_gained                        | c.4660C>T                | p.Gln1554*                   | .         |
|          |           | <i>PTPRT</i>   | chr20 | 41419837  | G              | A             | stop_gained                        | c.484C>T                 | p.Gln162*                    | .         |
|          |           | <i>MYH9</i>    | chr22 | 36710279  | G              | A             | stop_gained                        | c.1465C>T                | p.Gln489*                    | .         |
|          |           | <i>WAS</i>     | chrX  | 48547170  | ACC            | AC            | frameshift_variant                 | c.1058delC               | p.Pro353fs                   | .         |
|          |           | <i>PDE4DIP</i> | chr1  | 144916676 | C              | T             | stop_gained                        | c.1679G>A                | p.Trp560*                    | .         |
|          |           | <i>SOX11</i>   | chr2  | 5833426   | CG             | C             | frameshift_variant                 | c.578delG                | p.Gly193fs                   | .         |
|          |           | <i>FLT4</i>    | chr5  | 180046035 | A              | AG            | frameshift_variant                 | c.2835dupC               | p.Phe946fs                   | .         |
|          |           | <i>EGFR</i>    | chr7  | 55249012  | C              | CGGG<br>TTT   | conservative_<br>inframe_insertion | c.2310_2311ins<br>GGGTTT | p.Asp770_Asn<br>771insGlyPhe | COSM12378 |
|          |           | <i>XPA</i>     | chr9  | 100437714 | TAAA<br>AAAT   | TAAAA<br>AAAT | frameshift_variant                 | c.822_*1insT             | .                            | .         |
|          |           | <i>EP400</i>   | chr12 | 132547091 | CAA            | CA            | frameshift_variant                 | c.8181delA               | p.Gln2727fs                  | .         |
| 17       | SCC       | <i>TP53</i>    | chr17 | 7574012   | C              | A             | stop_gained                        | c.1015G>T                | p.Glu339*                    | COSM11286 |
|          |           | <i>TP53</i>    | chr17 | 7579470   | CGG            | CG            | frameshift_variant                 | c.215delC                | p.Val73fs                    | COSM46307 |
|          |           | <i>NF1</i>     | chr17 | 29553477  | ACCCC<br>CCCCG | ACCC<br>CCCCG | frameshift_variant                 | c.2033delC               | p.Pro678fs                   | COSM24489 |
|          |           | <i>COL1A1</i>  | chr17 | 48266813  | AC             | ATC           | frameshift_variant                 | c.2753_2754insA          | p.Pro919fs                   | .         |
|          |           | <i>CYP2D6</i>  | chr22 | 42524213  | C              | CG            | frameshift_variant                 | c.805dupC                | p.Arg269fs                   | .         |
|          | IP        | <i>PDE4DIP</i> | chr1  | 144916676 | C              | T             | stop_gained                        | c.1679G>A                | p.Trp560*                    | .         |
|          |           | <i>EGFR</i>    | chr7  | 55249012  | C              | CGGG<br>TTT   | conservative_<br>inframe_insertion | c.2310_2311ins<br>GGGTTT | p.Asp770_Asn<br>771insGlyPhe | COSM12378 |

Table IV. Continued

Table IV. *Continued*

| Case no. | Histology | Gene name     | Chrom | Position  | Reference | Alteration | Annotation         | HGVS.c          | HGVS.p      | COSMIC ID |
|----------|-----------|---------------|-------|-----------|-----------|------------|--------------------|-----------------|-------------|-----------|
|          |           | <i>CDKN2A</i> | chr9  | 21971193  | GC        | G          | frameshift_variant | c.164delG       | p.Gly55fs   | .         |
|          |           | <i>KMT2D</i>  | chr12 | 49445187  | T         | TC         | frameshift_variant | c.2278_2279insG | p.His760fs  | .         |
|          |           | <i>EP400</i>  | chr12 | 132547091 | CAA       | CA         | frameshift_variant | c.8181delA      | p.Gln2727fs | .         |
|          |           | <i>TP53</i>   | chr17 | 7579470   | CGG       | CG         | frameshift_variant | c.215delC       | p.Val73fs   | COSM46307 |
|          |           | <i>NF1</i>    | chr17 | 29553477  | ACCCC     | ACCCC      | frameshift_variant | c.2033delC      | p.Pro678fs  | COSM24489 |
|          |           |               |       |           | CCCCG     | CCG        |                    |                 |             |           |
|          |           | <i>CEBPA</i>  | chr19 | 33793213  | GCCCC     | GCCC       | frameshift_variant | c.209delG       | p.Gly71fs   | COSM18495 |

*ATRX*: ATRX chromatin remodeler; *CDKN2A*: cyclin-dependent kinase inhibitor 2A; *CEBPA*: CCAAT enhancer binding protein alpha; *COL1A1*: collagen type I alpha 1 chain; *CREBBP*: CREB-binding protein; *CYP2D6*: cytochrome P450 family 2 subfamily D member 6; *EGFR*: epidermal growth factor receptor; *EP400*: E1A-binding protein p400; *FLT4*: fms-related receptor tyrosine kinase 4; *FN1*: fibronectin 1; *GATA2*: GATA-binding protein 2; *IGF2*: insulin-like growth factor 2; *ITGA10*: integrin subunit alpha 10; *ITGB2*: integrin subunit beta 2; *KMT2D*: lysine methyltransferase 2D; *MPL*: MPL proto-oncogene, thrombopoietin receptor; *MYH11*: myosin heavy chain 11; *MYH9*: myosin heavy chain 9; *NF1*: neurofibromin 1; *NFKB2*: nuclear factor kappa B subunit 2; *PARP1*: poly(ADP-ribose) polymerase 1; *PDE4DIP*: phosphodiesterase 4D-interacting protein; *PKHD1*: PKHD1 ciliary IPT domain-containing fibrocystin/polyductin; *POU5F1*: POU class 5 homeobox 1; *PRKDC*: protein kinase, DNA-activated, catalytic subunit; *PTCH1*: patched 1; *PTPRT*: protein tyrosine phosphatase receptor type T; *SOC1*: suppressor of cytokine signaling 1; *SOX11*: SRY-box transcription factor 11; *TAF1*: TATA-box binding protein-associated factor 1; *TAFIL*: TATA-box binding protein associated factor 1-like; *TALI*: TAL bHLH transcription factor 1, erythroid differentiation factor; *TNK2*: tyrosine kinase non receptor 2; *TP53*: tumor protein p53; *TRRAP*: transformation/transcription domain-associated protein; *WAS*: WASP actin nucleation-promoting factor; *WHSC1*: Wolf-Hirschhorn syndrome candidate 1; *XPA*: XPA, DNA damage recognition and repair factor; *HGVS.c*: variants for a coding DNA sequence according to Human Genome Variation Society (HGVS); *HGVS.p*: variants for a protein sequence according to HGVS.

Malignant transformation of nasal papilloma-derived carcinoma is thought to be caused by the accumulation of genetic abnormalities in SNIP (5). *EGFR* mutation has been reported as one of the most important potential mechanisms of papilloma-derived carcinogenesis (16, 20, 22). In this study, *EGFR* mutations were found in two out of four patients with cancer. One patient also had a mutation in the IP. In nasal papilloma, *EGFR* mutations have been reported to be present in 20-91.4% of cases (14, 16, 20, 23). On the other hand, *EGFR* mutations in papilloma-derived cancer have been reported in 27-92.9% of cases. This suggests that *EGFR* may be an important factor at the time of papilloma development; however, it may not be important for malignant transformation from papilloma to cancer. Among those with papilloma-derived cancer, cases with *EGFR* mutations are reported to have a poorer prognosis in comparison to those without mutation, suggesting that *EGFR* may not be related to the grade of the cancer itself (23).

*TP53* is the most well-known tumor-suppressor gene. Immunostaining studies have shown a higher rate of *TP53* positivity in SNIP derived-SCC than in IP, suggesting that it may be important for transformation (5, 15). In the present study, we observed one case in which a *TP53* mutation was common to both the papilloma and the carcinoma of origin, and one additional mutation in the cancerous region. *TP53* is known to be inactivated by loss of heterozygosity or double mutation of the mutant allele. In this case, the double mutation may have occurred during the evolution from papilloma to carcinoma, resulting in the loss of *TP53* function (18, 24, 25).

Further studies are required because these findings were only observed in one case; however, malignant transformation may have occurred due to the gradual inactivation of *TP53* during IP-to-SCC transformation.

One limitation of this study is the small sample size of four cases and six samples. It is possible additional related genes might be identified by increasing the number of samples. Furthermore, case 16 did not have any mutations common to the SCC and IP parts of the sample. It is possible that SNIP and SNIP-derived SCC may have occurred simultaneously in this case, with completely different genetic backgrounds, or they may only share genes that were not analyzed in this study. Although this study analyzed mutations in 409 genes that have not previously been analyzed, a more comprehensive analysis of the entire exon sequence may be useful to determine whether a common mutation exists in this case.

## Conflicts of Interest

The Authors declare that no potential conflicts of interest exist in relation to this study.

## Authors' Contributions

RU and RY designed the study. RJ, HY and TH performed the experiments. RU performed the analysis and wrote the draft of the article. RU, RY, HY and TN reviewed and edited the article. TM, KS, KH, TH and TW performed collection of cases. All Authors read and approved the final article.

# Acknowledgements

This work was supported, in part, by the following grants and foundations: JSPS KAKENHI 17K16923 and 20K09757

# References

- 1 Leoncini G and Zanetti L: The papillomas of the sinonasal tract. A comprehensive review. *Pathologica* 109(1): 31-34, 2017. PMID: 28635991.
- 2 Goudakos JK, Blioukas S, Nikolaou A, Vlachtsis K, Karkos P and Markou KD: Endoscopic resection of sinonasal inverted papilloma: Systematic review and meta-analysis. *Am J Rhinol Allergy* 32(3): 167-174, 2018. PMID: 29649889. DOI: 10.1177/1945892418765004
- 3 Buchwald C, Franzmann M-B and Tos M: Sinonasal papillomas: A report of 82 cases in Copenhagen county, including a longitudinal epidemiological and clinical study. *Laryngoscope* 105(1): 72-79, 1995. PMID: 7837917. DOI: 10.1288/00005537-199501000-00016
- 4 Anari S and Carrie S: Sinonasal inverted papilloma: Narrative review. *J Laryngol Otol* 124(7): 705-715, 2010. PMID: 20388243. DOI: 10.1017/s0022215110000599
- 5 Re M, Gioacchini FM, Bajraktari A, Tomasetti M, Kaleci S, Rubini C, Bertini A, Magliulo G and Pasquini E: Malignant transformation of sinonasal inverted papilloma and related genetic alterations: A systematic review. *Eur Arch Otorhinolaryngol* 274(8): 2991-3000, 2017. PMID: 28432463. DOI: 10.1007/s00405-017-4571-2
- 6 Kim D-Y, Hong S-L, Lee CH, Jin H-R, Kang JM, Lee B-J, Moon IJ, Chung S-K, Rha K-S, Cho SH, Kim KR, Kim SW, Kim DW, Chung Y-J, Kim K-S, Won T-B, Shim WS, Park CH, Kang IG and Roh H-J: Inverted papilloma of the nasal cavity and paranasal sinuses: A Korean multicenter study. *Laryngoscope* 122(3): 487-494, 2012. PMID: 22253070. DOI: 10.1002/lary.22495
- 7 Mirza S, Bradley PJ, Acharya A, Stacey M and Jones NS: Sinonasal inverted papillomas: Recurrence, and synchronous and metachronous malignancy. *J Laryngol Otol* 121(9): 857-864, 2007. PMID: 17319993. DOI: 10.1017/s002221510700624x
- 8 Wu Y-H, Liang Q-Z, Li D-Z, Wang X-L, Huang H and Xu Z-G: Survival outcome of squamous cell carcinoma arising from sinonasal inverted papilloma. *Chin Med J* 128(18): 2457-2461, 2015. PMID: 32354352. DOI: 10.4103/0366-6999.164929
- 9 Long C, Jabarin B, Harvey A, Ham J, Javier A, Janjua A and Thamboo A: Clinical evidence-based review and systematic scientific review in the identification of malignant transformation of inverted papilloma. *J Otolaryngol Head Neck Surg* 49(1): 25, 2020. PMID: 32354352. DOI: 10.1186/s40463-020-00420-x
- 10 Yasumatsu R, Jiromaru R, Hongo T, Uchi R, Wakasaki T, Matsuo M, Taura M and Nakagawa T: A clinical analysis of sinonasal squamous cell carcinoma: A comparison of *de novo* squamous cell carcinoma and squamous cell carcinoma arising from inverted papilloma. *Acta Otolaryngol* 140(8): 706-711, 2020. PMID: 32400256. DOI: 10.1080/00016489.2020.1758342
- 11 Zhang L, Fang G, Yu W, Yang B, Wang C and Zhang L: Prediction of malignant sinonasal inverted papilloma transformation by preoperative computed tomography and magnetic resonance imaging. *Rhinology* 58(3): 248-256, 2020. PMID: 32441707. DOI: 10.4193/Rhin19.240
- 12 Yan CH, Tong CCL, Penta M, Patel VS, Palmer JN, Adappa ND, Nayak JV, Hwang PH and Patel ZM: Imaging predictors for malignant transformation of inverted papilloma. *Laryngoscope* 129(4): 777-782, 2019. PMID: 30515841. DOI: 10.1002/lary.27582
- 13 Lin GC, Scheel A, Akkina S, Chinn S, Graham M, Komarck C, Walline H, McHugh JB, Prince ME, Carey TE and Zacharek MA: Epidermal growth factor receptor, p16, cyclin d1, and p53 staining patterns for inverted papilloma. *Int Forum Allergy Rhinol* 3(11): 885-889, 2013. PMID: 24039221. DOI: 10.1002/alr.21215
- 14 Maisch S, Mueller SK, Traxdorf M, Weyerer V, Stoeck R, Iro H, Hartmann A and Agaimy A: Sinonasal papillomas: A single centre experience on 137 cases with emphasis on malignant transformation and *EGFR/KRAS* status in "carcinoma ex papilloma". *Ann Diagn Pathol* 46: 151504, 2020. PMID: 32203683. DOI: 10.1016/j.anndiagpath.2020.151504
- 15 Oncel S, Cosgul T, Calli A, Calli C and Pinar E: Evaluation of p53, p63, p21, p27, Ki-67 in paranasal sinus squamous cell carcinoma and inverted papilloma. *Indian J Otolaryngol Head Neck Surg* 63(2): 172-177, 2011. PMID: 22468256. DOI: 10.1007/s12070-011-0252-4
- 16 Udager AM, McHugh JB, Goudsmit CM, Weigelin HC, Lim MS, Elenitoba-Johnson KSJ, Betz BL, Carey TE and Brown NA: Human papillomavirus (HPV) and somatic *EGFR* mutations are essential, mutually exclusive oncogenic mechanisms for inverted sinonasal papillomas and associated sinonasal squamous cell carcinomas. *Ann Oncol* 29(2): 466-471, 2018. PMID: 29145573. DOI: 10.1093/annonc/mdx736
- 17 Yasukawa S, Kano S, Hatakeyama H, Nakamaru Y, Takagi D, Mizumachi T, Suzuki M, Suzuki T, Nakazono A, Tanaka S, Nishihara H and Homma A: Genetic mutation analysis of the malignant transformation of sinonasal inverted papilloma by targeted amplicon sequencing. *Int J Clin Oncol* 23(5): 835-843, 2018. PMID: 29779136. DOI: 10.1007/s10147-018-1296-1
- 18 Saito T, Niida A, Uchi R, Hirata H, Komatsu H, Sakimura S, Hayashi S, Nambara S, Kuroda Y, Ito S, Eguchi H, Masuda T, Sugimachi K, Tobo T, Nishida H, Daa T, Chiba K, Shiraishi Y, Yoshizato T, Kodama M, Okimoto T, Mizukami K, Ogawa R, Okamoto K, Shuto M, Fukuda K, Matsui Y, Shimamura T, Hasegawa T, Doki Y, Nagayama S, Yamada K, Kato M, Shibata T, Mori M, Aburatani H, Murakami K, Suzuki Y, Ogawa S, Miyano S and Mimori K: A temporal shift of the evolutionary principle shaping intratumor heterogeneity in colorectal cancer. *Nature Communications* 9(1), Nat Commun 9(1): 2884, 2018. PMID: 30038269. DOI: 10.1038/s41467-018-05226-0
- 19 Cingolani P, Platts A, Wang le L, Coon M, Nguyen T, Wang L, Land SJ, Lu X and Ruden DM: A program for annotating and predicting the effects of single nucleotide polymorphisms, SNPEff: SNPs in the genome of *Drosophila melanogaster* strain w1118; iso-2; iso-3. *Fly* 6(2): 80-92, 2012. PMID: 22728672. DOI: 10.4161/fly.19695
- 20 Udager AM, Rolland DCM, McHugh JB, Betz BL, Murga-Zamalloa C, Carey TE, Marentette LJ, Hermesen MA, Duross KE, Lim MS, Elenitoba-Johnson KSJ and Brown NA: High-frequency targetable *EGFR* mutations in sinonasal squamous cell carcinomas arising from inverted sinonasal papilloma. *Cancer Res* 75(13): 2600-2606, 2015. PMID: 25931286. DOI: 10.1158/0008-5472.can-15-0340

- 21 Cancer Genome Atlas Network: Comprehensive genomic characterization of head and neck squamous cell carcinomas. *Nature* 517(7536): 576-582, 2015. PMID: 25631445. DOI: 10.1038/nature14129
- 22 Hongo T, Yamamoto H, Jiromaru R, Nozaki Y, Yasumatsu R, Hashimoto K, Yoneda R, Sugii A, Taguchi K, Masuda M, Nakagawa T and Oda Y: Clinicopathologic significance of *EGFR* mutation and *HPV* infection in sinonasal squamous cell carcinoma. *Am J Surg Pathol*, 2020. PMID: 32868526. DOI: 10.1097/pas.0000000000001566
- 23 Sasaki E, Nishikawa D, Hanai N, Hasegawa Y and Yatabe Y: Sinonasal squamous cell carcinoma and *EGFR* mutations: A molecular footprint of a benign lesion. *Histopathology* 73(6): 953-962, 2018. PMID: 30117182. DOI: 10.1111/his.13732
- 24 Vogelstein B, Fearon E, Kern S, Hamilton, Preisinger A, Nakamura Y and White R: Allelotype of colorectal carcinomas. *Science* 244(4901): 207-211, 1989. PMID: 2565047. DOI: 10.1126/science.2565047
- 25 Sawada G, Niida A, Uchi R, Hirata H, Shimamura T, Suzuki Y, Shiraishi Y, Chiba K, Imoto S, Takahashi Y, Iwaya T, Sudo T, Hayashi T, Takai H, Kawasaki Y, Matsukawa T, Eguchi H, Sugimachi K, Tanaka F, Suzuki H, Yamamoto K, Ishii H, Shimizu M, Yamazaki H, Yamazaki M, Tachimori Y, Kajiyama Y, Natsugoe S, Fujita H, Mafune K, Tanaka Y, Kelsell DP, Scott CA, Tsuji S, Yachida S, Shibata T, Sugano S, Doki Y, Akiyama T, Aburatani H, Ogawa S, Miyano S, Mori M and Mimori K: Genomic landscape of esophageal squamous cell carcinoma in a Japanese population. *Gastroenterology* 150(5): 1171-1182, 2016. PMID: 26873401. DOI: 10.1053/j.gastro.2016.01.035
- 26 Brierley J, Gospodarowicz MK and Wittekind C (eds.): *TNM Classification of Malignant Tumours*. J Wiley & Sons, Hoboken, NJ, USA.

*Received November 3, 2020*

*Revised November 19, 2020*

*Accepted November 20, 2020*